Ecological Engineering 138 (2019) 444–453

Contents lists available at ScienceDirect

Ecological Engineering

journal homepage: www.elsevier.com/locate/ecoleng

Hydrogen peroxide measurements in subtropical aquatic systems and their implications for cyanobacterial blooms

Luka K. Ndungu[a], Jacob H. Steele[a], Taylor L. Hancock[a], Richard D. Bartleson[b], Eric C. Milbrandt[b], Michael L. Parsons[a], Hidetoshi Urakawa[a,*]

[a] Department of Marine and Ecological Sciences, Florida Gulf Coast University, Fort Myers, FL 33965, USA
[b] Marine Laboratory, Sanibel-Captiva Conservation Foundation, Sanibel, FL 33957, USA

ARTICLE INFO

Keywords:
Caloosahatchee River
Cyanobacteria
Florida
Freshwater
Harmful algal bloom (HAB)
Hydrogen peroxide
Microcystin
Microcystis aeruginosa
Rainwater
Reactive oxygen species (ROS)

ABSTRACT

Hydrogen peroxide is widely recognized as the most stable of the reactive oxygen species (ROS) produced by both biotic and abiotic pathways in natural waters. Its high reactivity in mediating redox transformations may, directly or indirectly, affect aquatic ecosystem functions, including primary productivity. However, environmental interactions between photoautotrophs, particularly cyanobacteria, and hydrogen peroxide are poorly understood. To gain a better understanding of hydrogen peroxide and cyanobacterial interactions, we determined the hydrogen peroxide concentrations in the presence and absence of cyanobacterial blooms in southwest Florida. Hydrogen peroxide concentrations were determined using a fast response amperometric hydrogen peroxide microelectrode. Our measurements ranged from 0 to 5.3 μM in freshwater bodies (ponds, lakes and the Caloosahatchee River) and 0 to 92.9 μM in rainwater. In general, hydrogen peroxide levels were highly associated with cyanobacterial bloom conditions, indicating the potential role of cyanobacteria in hydrogen peroxide production in freshwater. To determine the potential biodegradation of hydrogen peroxide during sample transportation in the dark condition, water samples were passed through 0.2 μm pore size filters immediately after sampling and compared with unfiltered water samples in the laboratory. We found that filtered water samples retained higher concentrations of hydrogen peroxide than unfiltered samples with a mean biodegradation rate of 44 ± 10.6 nmol/h. Out of a total of 26 samples, only one unfiltered sample showed a higher hydrogen peroxide concentration than the filtered samples. Overall, our study found the microelectrode technique could accurately measure hydrogen peroxide concentrations in the samples from various freshwater bodies. This measurement method revealed that hydrogen peroxide concentrations vary with temporal and spatial dynamics of cyanobacterial blooms.

1. Introduction

Hydrogen peroxide, being one of the most stable and abundant forms of reactive oxygen species (ROS) in aquatic ecosystems, has long been documented as an unwanted toxic byproduct produced during normal metabolism by endogenous processes of aquatic organisms; and by photochemical processes in natural water bodies (Cooper et al., 1988; Scully et al., 1996; Petasne and Zika, 1997). In addition, atmospheric wet deposition has also been found to be a source of hydrogen peroxide to aquatic ecosystems (Cooper et al., 1987; Kang et al., 2002). ROS including hydrogen peroxide and superoxide (O^{2-}) are highly reactive and are produced as intermediates during the sequential one-electron reduction of oxygen to water. ROS have the ability to interact with biologically pivotal metals such as iron, copper, and manganese (Nico et al., 2002; Rose et al., 2008). This high reactivity in mediating redox transformations may, directly and indirectly, affect aquatic biota and ecosystems. This is particularly important for cyanobacteria since recent studies emphasize the implications of iron and cyanobacterial blooms in the open ocean (Bowie et al., 2009) as well as nutrient-rich freshwater bodies (Xing et al., 2014). The photosynthetic production of hydrogen peroxide from cyanobacteria has been reported under laboratory conditions (Patterson and Myers, 1973; Roncel et al., 1989). However, knowledge about the environmental interaction between cyanobacteria and naturally-occurring levels of hydrogen peroxide is limited (Mostofa et al., 2013; Pflaumer, 2016).

To understand hydrogen peroxide dynamics and the interaction of hydrogen peroxide with cyanobacterial blooms, we aimed to determine the hydrogen peroxide levels present in the freshwater environments in

* Corresponding author at: Florida Gulf Coast University, 10501 FGCU Blvd. S., Fort Myers, FL 33965, USA.
E-mail address: hurakawa@fgcu.edu (H. Urakawa).

https://doi.org/10.1016/j.ecoleng.2019.07.011
Received 27 March 2019; Received in revised form 16 June 2019; Accepted 9 July 2019

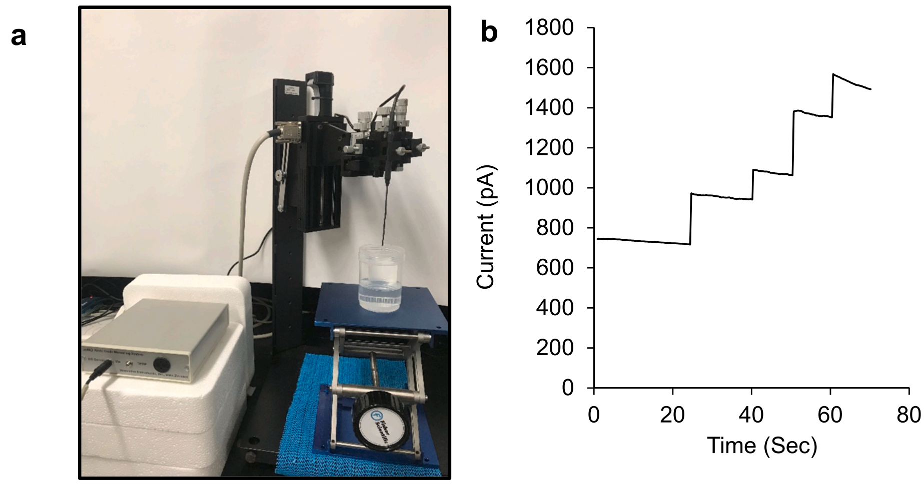

Fig. 1. Performance evaluation of a hydrogen peroxide microelectrode. (a) 250 µm tip diameter hydrogen peroxide microelectrode with a built-in reference electrode. (b) The microelectrode linearly reacted with the repetitive addition (x4) of 50 nM of hydrogen peroxide.

the presence and absence of cyanobacterial blooms in southwest Florida during the wet season and assessed abiotic factors that potentially contribute to the generation and degradation of hydrogen peroxide.

2. Materials and methods

2.1. Hydrogen peroxide quantification using a microelectrode

We used a recently developed fast response amperometric 250 µm diameter tip hydrogen peroxide microelectrode with a built-in reference electrode (HP-250, Innovative Instruments, Inc., Tampa, FL, USA) featuring a lower detection limit of 50 nM (Fig. 1). The sensor was connected to an inNO-T meter operated by the inNO-T data acquisition system software (Innovative Instruments, Tampa, FL, USA) on a personal computer. Hydrogen peroxide (3% w/v) was purchased from Sigma-Aldrich (St. Louis, MO, USA) and used in the preparation of standard curves. Before calibration, the condition of the sensor was monitored via readings in the air and in high-performance liquid chromatography (HPLC) grade water. The sensor system was run for at least 20 min in HPLC grade water before measurements to establish a stable background baseline. At least six replicate readings were recorded and used to calculate the mean and standard error of each measurement.

2.2. Hydrogen peroxide quantification using ferrous oxidation/xylenol orange method

Hydrogen peroxide concentrations were also determined using a method of ferrous oxidation in the presence of xylenol orange (Pierce Quantitative Peroxide Assays, Pierce Biotechnology, Rockford, IL, USA). A fresh working solution was prepared for each experiment, and each working solution was <30 min old when it was used. Reagents together with samples were incubated for 15–20 min before reading on a microtiter plate at 590 nm using a TECAN Genios Pro 96 multifunction microplate reader (MTX Lab Systems, Bradenton, FL, USA).

2.3. Lake water sample collections

From March 2017 to July 2018, surface water samples were collected from various oligotrophic to hypertrophic water bodies in southwest Florida (Fig. 2). Physiochemical parameters such as water temperature, pH, dissolved oxygen (DO), and electrical conductivity were measured using a YSI sonde (Yellow Springs, OH, USA). To measure the chlorophyll *a* concentration, the water samples (50 mL) were filtered using a GF/F filter (0.7 µm pore size, 25 mm diameter, Whatman), extracted with 90% acetone and quantified using a Trilogy Laboratory Fluorometer (Turner Designs, San Jose, CA, USA) with chlorophyll acid module CHL-A-ACID (Model 7200–040). Phaeophytin concentrations were determined after the acidification of samples with 1 N HCl (Holm-Hansen et al., 1965). Colored dissolved organic matter (CDOM) and turbidity were measured in a 3.5 mL cuvette as triplicates on the same fluorometer with different modules, CDOM/NH4 (Model 7200–041) and TURBIDITY (Model 7200–060), respectively.

2.4. Hydrogen peroxide in rainwater

Rainwater samples were collected during the rainy seasons in 2017 to 2018 on the Florida Gulf Coast University (FGCU) campus using a 10% HCl acid-washed plastic funnel in a 1 L polypropylene bottle placed on open ground 20 m away from building and vegetation (Fig. 2). The samples were analyzed using the hydrogen peroxide microelectrode within 24 h of sample collection. Catalase of *Aspergillus niger* (100 U/mL as final concentration, Merck Millipore, Billerica, MA, USA) was used to confirm if detected high sensor signals in rainwater samples were true responses to hydrogen peroxide, using a similar approach to that of Eberhardt et al. (2004).

2.5. Hydrogen peroxide decay measurements

Filtered and unfiltered water samples were used to assess the potential degradation of hydrogen peroxide during the transportation of samples to the laboratory from the field (a trip of approximately two hours). Water samples were collected using a clean 50 mL graduated polypropylene screw-capped centrifuge tube followed by filtering through a 25 mm diameter 0.2 µm pore size polycarbonate filter (GTTP, Millipore Sigma, St. Louis, MO, USA). All water samples were placed on blue ice and transported to the laboratory and analyzed within 6 h.

2.6. Iron measurements in water samples and cyanobacterial biomass

Total iron, both particulate and dissolved species, was determined from the fresh and frozen samples. Ten-milliliter aliquots of water samples were transferred into acid-washed 15 mL graduated polypropylene screw-capped centrifuge tubes. Total iron was quantified using the United States Environmental Protection Agency (US EPA) approved 1, 10 phenanthroline method (FerroVer Iron Reagent Powder Pillows, HACH, Loveland, CO, USA). Total iron concentrations were determined for unfiltered water samples. Intracellular iron concentrations in cyanobacterial biomass were determined by subtraction of the concentration of the filtered fraction from the total iron concentration.

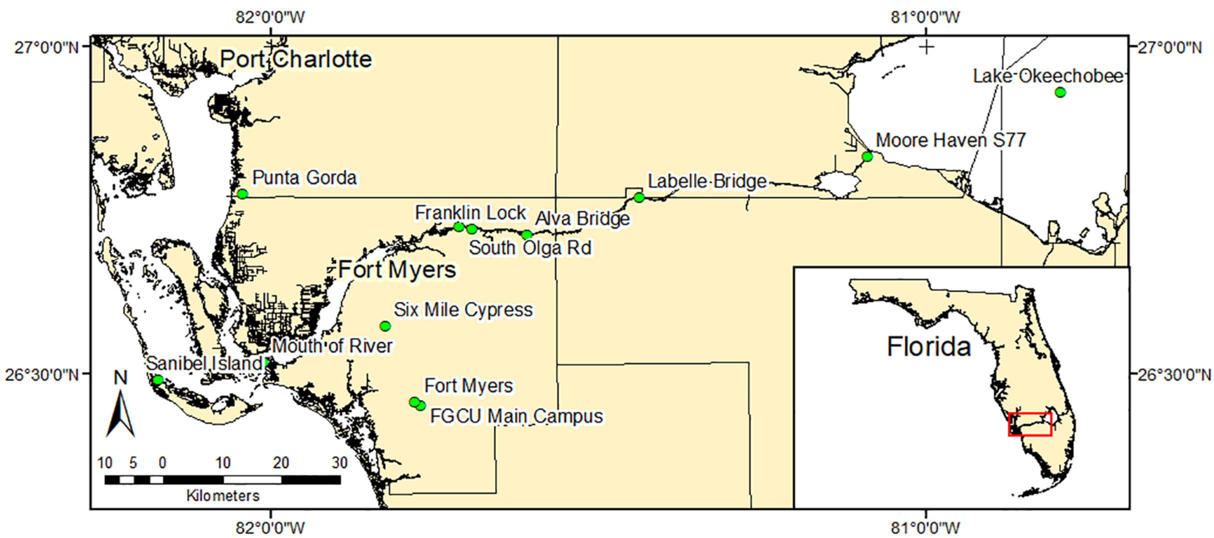

Fig. 2. Southwest Florida map showing the locations where the samples were collected in 2017 and 2018.

Water samples including cyanobacterial scums were gently filtered with a 25 mm Whatman GF/F filter and a hand-held vacuum pump to avoid mechanical disruption of cyanobacterial cells. The iron concentrations were colorimetrically determined using a HACH DR/2400 Spectrophotometer (Loveland, CO, USA) at a wavelength of 590 nm.

2.7. Nutrient analyses

Water samples were prepared by filtering 50 mL of the sample through a 45 mm diameter Whatman GF/F glass fiber filter and stored at −20 °C until analysis. All nutrient analyses were performed using a Seal Analytical Discrete Analyzer Model AQ2 (SEAL Analytical, Mequon, WI, USA) following US EPA Standard Methods protocols. Total phosphorus (TP) and total nitrogen (TN) were determined after digestion (20 min at 120 °C) using an autoclave. Nutrients were determined as follows: orthophosphate (ascorbic acid method 4500-PE), ammonia (phenate method 4500-NH_3-G), nitrite (diazotizing with sulfanilamide and NED dihydrochloride method 4500-NO_2-B) and NOx (cadmium reduction method 4500-NO_3-E). Nitrate was determined by subtracting nitrite from NOx.

2.8. Quantification of microcystins using ELISA test kit

Surface water samples containing scum of cyanobacteria were collected from Lake San Carlos (Oct 31, Nov 8 and Dec 6, 2017), Devitt Lake (Sep 28, 2017) and the Caloosahatchee River (Jun 28, 2018) and were used to evaluate cyanotoxin concentrations (Fig. 2). The water samples were treated with three freeze–thaw cycles to induce cell lysis (US EPA method 546). After cell lysis, samples were centrifuged at 4000 × *g* for 1 min, and the resulting supernatants were transferred to new centrifuge tubes for microcystin analysis. The total concentration of microcystin-LR was determined using an ELISA test kit (Beacon Microcystin Tube Kit, Beacon Analytical Systems, ME, USA) according to the manufacturer's instructions. The test kit uses a polyclonal antibody (anti-rabbit IgG) to bind both microcystins and a microcystin-enzyme conjugate. The ELISA assay induced color changes from dark to pale blue in relation to the different concentrations of microcystin, and was measured using a spectrophotometer at a wavelength of 450 nm (Genesys 20 Thermo Scientific, Waltham, MA). It should be noted that the ELISA test kit used is approved in US EPA method 546 and optimized to detect microcystin-LR but cannot completely discriminate different types of microcystins (e.g., LA, YR or RR).

2.9. Data analysis

General statistics were calculated for biotic and abiotic data sets using the Data Analysis Tools in Microsoft Excel. The majority of data were presented as mean ± one standard error unless denoted. Regression analyses were performed between two variables of interest. Pearson's correlation was calculated to determine significant relationships between biotic and abiotic parameters.

3. Results

3.1. Hydrogen peroxide concentration in aquatic systems in southwest Florida

The hydrogen peroxide measurements obtained via microelectrode and xylenol orange methods were highly correlated with each other ($R = 0.99$, $P < 0.001$), but the microelectrode provided a higher sensitivity (down to 50 nM of hydrogen peroxide), which is more suitable to quantify hydrogen peroxide concentrations in field samples (Fig. 1). The mean concentration of hydrogen peroxide in rainwater was 16.8 ± 4.0 µM (mean ± SE, $n = 24$), with a range of 0 to 92.9 µM, which was similar to the previous reports (Table 1). Hydrogen peroxide in rainwater samples was decomposed to a level below limits of detection after catalase treatment, indicating that the sensor was truly responding to hydrogen peroxide in rainwater. Our hydrogen peroxide measurements of lake water varied in the range of 0 and 5.31 µM (Table 1). We found a lower range of hydrogen peroxide concentrations of 0.42 ± 0.07 µM ($n = 5$) in FGCU main campus ponds, which had lower nutrient levels (oligotrophic/mesotrophic) than the other field sites (Table 2). High levels of hydrogen peroxide were detected in the lakes and ponds in Six Mile Cypress Slough Preserve, a cypress wetland system that receives sheet flow groundwater and is normally low in nutrient concentrations (oligotrophic) except for Gator Lake (mesotrophic) where cyanobacterial blooms are occasionally documented (Urakawa and Bernhard, 2017). When we collected water samples in May 2016, southwest Florida had experienced extremely dry conditions due to an El Niño event (Yeoman et al., 2017). The water level was extremely low (< 30 cm), and a high chlorophyll *a* concentration was detected along with high hydrogen peroxide concentrations (Table 2). A high level of hydrogen peroxide was detected in Gator Lake in which a cyanobacterial bloom had developed (Fig. 3a). Negative correlations were found between hydrogen peroxide concentrations (filtered and non-filtered) and water temperature (Table 3).

Table 1
The typical range of hydrogen peroxide concentrations in aquatic systems.

Aquatic system	Reference	Detected range of hydrogen peroxide (μM)	
		Low	High
River	Cooper and Zika (1983)	0.09	0.80
	Sinel'nikov (1971)	1.30	3.20
Lake	Cooper and Lean (1992)	0.01	0.80
	Häkkinen et al. (2004)	0.03	1.04
	Cooper and Lean (1989)	0.01	0.80
	Cory et al. (2016)	0.05	1.57
	This Study*	**0.00**	**5.31**
Estuary	Fujiwara et al. (1995)	0.06	0.14
	Kieber and Helz (1995)	0.01	0.35
	Amouroux and Donard (1995)	0.02	0.26
	Miller et al. (2005)	0.06	0.28
Open ocean	Olasehinde et al. (2008)	0.14	0.35
	Fujiwara et al. (1993)	0.06	0.45
Rain	Hellpointner and Gäb (1989)	2.30	110.6
	Cooper and Lean (1992)	8.40	82.0
	Sakugawa et al. (1990)	0.00	199.0
	This study	**0.00**	**92.9**

* Data from Summit Church were collected during a chemical treatment of pond for algal control and were not included.

3.2. Biodegradation of hydrogen peroxide during sample transportation

We found that the filtered water samples retained higher concentrations of hydrogen peroxide than non-filtered samples (Fig. 3a). Out of 26 samples, only one non-filtered sample showed a higher hydrogen peroxide concentration than filtered samples (Fig. 3a). The mean biodegradation rate of hydrogen peroxide was 44.7 ± 2.2 nmol/h, which was calculated based on the difference between filtered and non-filtered samples (Häkkinen et al., 2004; Richard et al., 2007).

3.3. Iron measurement in water samples and cyanobacterial biomass

Total iron concentrations in the southwest Florida lakes ranged from 0.02 to 4.56 mg/L (median = 0.29 mg/L). In both eutrophic and oligotrophic sites, we found a positive correlation between chlorophyll *a* and total iron concentrations ($R = 0.60$, $P = 0.001$, $n = 26$) (Fig. 4). Analysis of filtered and non-filtered samples that had high total chlorophyll concentrations (i.e., cyanobacterial blooms) showed that over half of the iron was in the cyanobacterial cells (65.2 ± 5.0%, mean ± SE, $n = 3$). No correlation was found between the filtered hydrogen peroxide samples and total iron concentrations ($R = 0.07$, $P = 0.73$, $n = 26$) (Table 3).

3.4. Cyanobacterial bloom and hydrogen peroxide

During the 2017 and 2018 *Microcystis* bloom event (June to November), we measured hydrogen peroxide and microcystin along with environmental parameters (Table 4). We found no correlation between hydrogen peroxide and microcystin concentrations ($R = 0.39$, $P = 0.38$, $n = 7$). The range of microcystin concentrations in the Caloosahatchee River was 0.04 – 451 μg/L with a mean of 112.96 ± 26.67 μg/L ($n = 7$), while the hydrogen peroxide ranged from 0.20 − 5.07 μM with a mean of 2.78 ± 0.26 μM ($n = 7$).

3.5. Cyanobacterial bloom events in Lake Okeechobee and the Caloosahatchee River in summer 2018

During the 2018 bloom, we tested microcystin concentrations in water samples from the Caloosahatchee River. We found microcystin concentrations of 450.5 μg/L at Fort Denaud Bridge and 308.1 μg/L at Alva Bridge (Table 4). Combined with microcystin data provided by the Florida Department of Environmental Protection (Florida Algal Bloom Sample Collection View), microcystin concentrations in the Caloosahatchee River ranged from 0 to 463.3 μg/L with a mean of 14.0 ± 3.6 ($n = 180$) (Fig. 5). The highest concentrations of microcystin (greater than 100 μg/L) were found from five locations, where the concentrations were well above the World Health Organization (WHO) health advisory level of < 20 μg/L for recreational waters (WHO, 2003) and < 1 μg/L for drinking water (WHO, 2004).

4. Discussion

Hydrogen peroxide is one of the most stable and abundant forms of reactive oxygen in aquatic ecosystems (Kieber et al., 2003; Diaz and Plummer, 2018). For decades, a variety of methods have been employed to quantify hydrogen peroxide concentrations in pharmaceutical, biological, clinical and environmental settings (Mostofa et al., 2013).

The classical hydrogen peroxide detection method is a colorimetric method used to determine concentrations in plant tissues. In this method, hydrogen peroxide is reacted with 4-aminoantipyrine and phenol to produce a stable red product in the presence of peroxidase (Patterson et al., 1984; Zhou et al., 2006). In freshwater lakes, hydrogen peroxide is determined using a spectrofluorometric method where the enzyme-catalyzed reaction between N-acetyl-3,7- dihydroxyphenoxazine (APOXA) and hydrogen peroxide forms a fluorescent product (Häkkinen et al., 2004; García et al., 2019). In rainwater, p-hydroxyphenylacetic acid (PHPA) has been used in a spectrophotometric method to determine hydrogen peroxide concentrations (Tanner and Wong, 1998; Shariati-Rad et al., 2015). Electrochemistry can determine small amounts of hydrogen peroxide utilizing o-dianisidine (ODA) as a substrate and hemoglobin as a catalyst (Sun et al., 2005). The electrochemical method used in the medical field has been shown to work for measuring hydrogen peroxide in rainwater (Sun et al., 2005). In surface waters, the presence of other ROS (superoxides, hydroxyl ions, free radicals, and singlet oxygen) has led to the development of a chromatography method that is capable of identifying peroxide separately from other ROS (Takahashi et al., 1999; Steinberg, 2013; Gimeno et al., 2015). A majority of these methods have had limited success due to their poor selectivity and sensitivity, long analysis time, and lack of long-term reliability and reproducibility.

The development of the hydrogen peroxide sensor has made hydrogen peroxide quantification easier because of the sensor's simplicity, rapidity, selectivity, high sensitivity and capability of providing real-time results (Urban et al., 2018). In this study, we applied hydrogen peroxide sensors both on-site and in the laboratory. To confirm the accuracy of our hydrogen peroxide measurements, we used two methods, a hydrogen peroxide microelectrode technique, and a ferrous oxidation/xylenol orange assay. Both methods correlated well with each other ($R = 0.99$, $P < 0.001$) but the sensor was more sensitive in the lower detection range and suitable for quantifying hydrogen peroxide concentration in both lake water and rainwater samples.

Hydrogen peroxide is ubiquitously found in both freshwater and marine environments with higher concentrations in freshwater (Kieber and Helz, 1995; Mostofa et al., 2013). Our hydrogen peroxide measurements of the lake, pond, and river water samples showed a broad concentration range (Table 1). Actually, the highest concentrations of hydrogen peroxide in pond water were found in Summit Church (12.95 μM at the non-bloom site and 16.50 μM at the bloom site) (Table 2). However, it should be noted that these pond water samples were collected after copper sulfate treatment conducted by the landowner. Further research is required to understand the interactions between hydrogen peroxide and algaecide treatments. Therefore, these high values were removed from the comparison of hydrogen peroxide concentrations in aquatic systems (Table 1).

Water temperature is indirectly dependent on solar irradiation and

Table 2
Hydrogen peroxide concentrations in filtered and non-filtered water samples and physicochemical parameters of water samples collected in southwest Florida.

Location	Coordinates	Date	Hydrogen peroxide (μM)		Temp	pH	Chl *a*	Pheo	DO	EC	Iron	Turb	CDOM
		m/d/y	filtered	non-filtered	(°C)		(μg/L)	(μg/L)	(mg/L)	(μS/cm)	(mg/L)	(NTU)	(mg/L)
Gator Lake	26°34′22″ N 81° 49′30″W	5/8/2017	4.53	4.90	26.2	8.0	5.9	4.6	2.8	514	0.13	6.9	0.18
Wood Duck Pond	26°34′33″N 81°49′22″ W	5/8/2017	5.07	1.33	29.3	8.3	30.3	14.8	5.8	756	0.84	23.2	0.18
Pop Ash Pond	26°34′25″ N 81°49′24″ W	5/8/2017	5.31	2.37	22.4	8.3	23.6	10.4	5.0	787	0.25	34.5	0.19
Otter Pond	26°34′20″ N 81°49′26 W	5/25/2017	4.46	1.81	30.1	9.1	54.9	69.1	8.2	802	0.30	154.8	0.17
Bike Trail Lake	26°26′10″N 82^{0} 6′30″W	5/24/2017	0.77	0.00	28.8	8.2	36.9	nd	4.0	8869	0.24	24.0	0.65
Sanctuary Lake	26^{0} 29′29″N 82^{0} 10′19″W	5/31/2017	2.34	0.66	32.7	8.9	49.6	nd	17.5	2574	0.38	20.2	0.61
Dunes Lake	26^{0} 27′8″N 82^{0} 2′29″W	5/31/2017	1.72	0.32	33.9	9.2	66.1	nd	16.7	5036	0.27	38.2	0.78
Gulf Coast Lake	26^{0} 26′30″N 82^{0} 3′3″W	5/31/2017	1.11	0.22	30.8	8.4	31.6	nd	9.8	2032	0.36	20.3	0.58
Pelican Lake	26°46′11″N 82°3′11″W	6/13/2017	0.36	0.00	29.0	7.9	1.4	0.4	6.3	4823	0.03	2.5	0.60
Kingfisher Lake	26°46′28″N 82°2′33″W	6/13/2017	1.64	0.28	29.5	9.3	2.2	0.8	10.7	1957	0.15	18.2	0.65
Osprey Lake	26°46′15″N 82°2′55″W	6/13/2017	0.35	0.00	30.4	7.9	1.7	0.3	6.6	13,590	0.02	4.6	0.65
Sovi Pond	26^{0}27′35″N 81^{0}45′59″W	7/5/2017	0.55	0.04	32.2	8.7	0.3	0.2	5.0	1730	0.69	4.7	0.56
Library Pond	26^{0}27′2″N 81^{0}46′15″W	7/5/2017	0.36	0.01	31.9	8.3	0.1	0.1	4.7	2030	0.40	4.9	0.52
Welcome Center Lake	26^{0}27′32″N 81^{0}46′25″W	7/5/2017	0.30	0.01	32.1	7.8	0.2	0.1	4.5	2250	0.61	5.1	0.53
Food Forest Pond	26^{0}27′37″N 81^{0}46′48″W	7/5/2017	0.28	0.05	34.4	7.4	0.4	0.1	2.4	1710	0.27	5.2	0.58
North Lake	2627′57″N 81^{0}46′8″W	7/5/2017	0.62	0.05	31.5	8.7	0.2	0.3	7.1	1890	0.08	5.5	0.59
Summit Church (no bloom site)	26^{0}27′22″N 81^{0}46′47″W	1/20/2018	12.95	9.46	16.7	8.1	0.4	0.1	7.6	420	0.82	11.3	0.48
Summit Church (bloom site)	26^{0}27′22″N 81^{0}46′47″W	1/20/2018	16.50	7.48	16.7	8.1	1.3	1.3	7.0	410	0.03	0.0	0.50
Lake San Carlos	26^{0}28′45″N 81^{0}49′7″W	10/31/2017	3.03	4.76	21.4	9.2	11.4	0.9	8.6	310	0.46	0.8	0.24
Punta Rassa (top)	26^{0}31′3″N 82^{0} 0′40″W	7/10/2017	0.76	0.00	31.2	7.9	1.7	0.4	5.8	43,766	0.03	2.9	0.31
Punta Rassa (bottom 1.5 m)	26^{0}31′3″N 82^{0} 0′40″W	7/10/2017	0.81	0.11	31.1	8.0	2.1	0.7	4.6	44,096	0.08	6.9	0.30
Twin Palm Drive (top)	26^{0}35′26″N 81^{0}53′50″W	7/10/2017	0.97	0.29	29.7	7.6	7.0	2.4	4.5	4807	0.23	3.8	0.35
Twin Palm Drive (bottom 1.2 m)	26^{0}35′26″N 81^{0}53′50″W	7/10/2017	1.01	0.40	30.1	7.6	3.8	2.6	3.8	5988	0.33	6.4	0.34
Alva Bridge	26^{0}42′45″N 81^{0}36′35″W	6/27/2018	0.83	0.00	31.0	7.1	100.7	0	1.6	112	2.43	1.8	0.50
Fort Denaud Bridge	26^{0}44′41″N 81^{0}30′37″W	6/27/2018	0.27	0.00	32.4	7.7	72.5	0	3.0	116	1.32	4.6	0.50
Rosen Park Cape Coral	26^{0}62′46″N 81^{0}92′37″W	7/24/2018	5.07	4.61	30.4	7.9	65.4	0	5.5	116	4.56	nd	nd

Abbreviations: Temp, temperature; Chl *a*, chlorophyll *a;* Pheo, pheophytin *a*; DO, dissolved oxygen; EC, electrical conductivity; Iron, total iron; Turb, turbidity; and CDOM, colored dissolved organic matter. nd, no data are available. The total iron and all water quality data measured by the YSI sensor are shown as the mean of triplicate measurements. The mean coefficient variation of total iron measurements was 16%. The mean coefficient variation of CDOM measurements was 8%. Hydrogen peroxide data represent the mean of six measurements. Chl *a* data are from a single measurement. Data from Summit Church were collected during a chemical treatment of pond for algal control. Punta Rassa, Twin Palm Drive, Alva Bridge, and Rosen Park in Cape Coral are sampling sites in the Caloosahatchee River.

the production of hydrogen peroxide in aquatic environments largely depends on the amount of dissolved organic matter and solar radiation (Mostofa et al., 2013). Therefore, global warming with the associated water temperature rise would enhance the production of hydrogen peroxide through the photodegradation of dissolved organic matter and photosynthesis activities (Mostofa et al., 2013). However, in the present study, negative correlations were found between hydrogen peroxide concentrations (filtered and non-filtered) and water temperature, indicating a potential effect of water temperature on hydrogen peroxide concentrations (Table 3). Water temperature influences both microbial activity and hydrogen peroxide degradation rates. However, these correlations were lost when data sets from Six Mile Cypress Slough Preserve, which have low water temperatures and high hydrogen peroxide levels, were removed. Thus, a further seasonal study is required to conclude the relationship between hydrogen peroxide concentrations and water temperatures.

Rainwater normally contains much higher concentrations of hydrogen peroxide than any other water source (Mostofa et al., 2013). Rainwater samples in southwest Florida had a mean hydrogen peroxide concentration of 16.8 ± 4.0 μM (mean ± SE, n = 24), within the reported range of rainwater (Sakugawa et al., 1990; Claiborn and Aneja, 1991; Kieber et al., 2001a,b) and this was greater than typical lake and

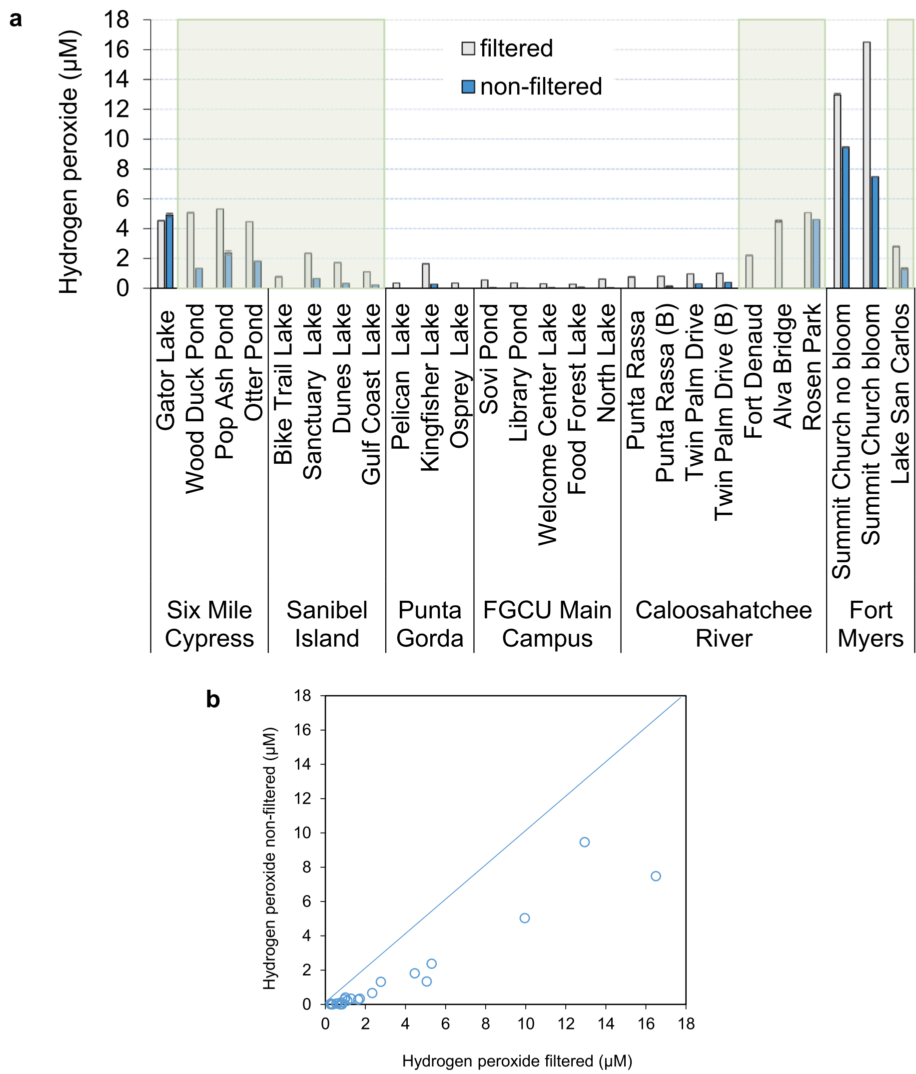

Fig. 3. The effect of filtration treatment on the hydrogen peroxide concentration of water samples. (a) The green areas represent the sites with chlorophyll *a* greater than 25 µg/L, which is a mean chlorophyll *a* concentration in Florida lakes reported previously (Bigham et al., 2009). Letter B represents bottom water. In Summit Church Pond, one site had a surface bloom while the other site had no bloom. Data represent mean and the standard deviation of six measurements. Note that error bars are very small. (b) Scatter plot of hydrogen peroxide concentrations from the filtered and non-filtered samples. The blue line shows a 1:1 relationship.

river water concentrations (Table 1). The majority of lakes and ponds visited in this study were created for stormwater detention, and as this research was conducted in the rainy season, rainwater runoff could be a major reason why the background level of hydrogen peroxide concentrations of our lake and pond water samples were higher than the other areas (Table 1). Cooper and Lean (1992) suggested that high dissolved organic matter and strong sunlight may stimulate the formation of ROS in surface waters of Florida.

The influence of biotic communities on the rate of hydrogen peroxide production/decomposition has been studied in freshwater (Häkkinen et al., 2004; Richard et al., 2007) and marine environments (Petasne and Zika, 1997). Lines of evidence suggest the contribution of

Table 3
Pearson's correlation of biotic and abiotic parameters.

	Filtered H_2O_2	Non-filtered H_2O_2	Temp	pH	Chl *a*	Pheo	DO	EC	Iron	Turb	CDOM
Filtered H_2O_2		**3.66E-10**	**5.46E-08**	0.70155	0.69877	0.61423	0.60455	0.23876	0.72558	0.14554	0.27415
Non-filtered H_2O_2	**0.90062**		**9.04E-09**	0.71837	0.59374	0.94159	0.84254	0.18975	0.35093	0.13916	0.13773
Temp	**−0.84541**	**−0.86829**		0.72963	0.20531	0.91209	0.86355	0.35233	0.65377	**0.042749**	0.10372
pH	0.078921	0.074281	−0.0712		0.94399	0.066059	**1.37E-05**	0.44724	0.18158	0.3715	0.70318
Chl *a*	−0.079691	−0.10969	0.25683	−0.01449		0.18464	0.43888	0.21944	**0.001167**	0.91681	0.68761
Pheo	0.11375	0.016589	0.024994	0.39871	0.29369		0.25327	0.57503	0.67323	0.5134	**0.022376**
DO	0.10651	0.040956	0.035437	**0.74306**	0.15865	0.25439		0.70661	0.34667	0.089506	0.068174
EC	−0.23944	−0.26558	0.19008	−0.1558	−0.24927	−0.12643	−0.07752		0.22328	0.20439	0.47879
Iron	0.072304	0.19062	0.092317	−0.27038	**0.60100**	−0.09527	−0.19229	−0.24727		0.1512	0.97967
Turb	−0.29969	−0.30429	**0.40828**	−0.18671	−0.02201	−0.15104	−0.34673	−0.26279	0.29574		0.18836
CDOM	−0.22747	−0.30535	0.3331	0.080189	0.084609	**−0.49547**	0.37063	−0.14846	−0.00537	0.27202	

See the abbreviations in Table 2. *P* is shown in the upper right and *r* is shown in the lower left. Significant values ($p < 0.05$) are shown in bold.

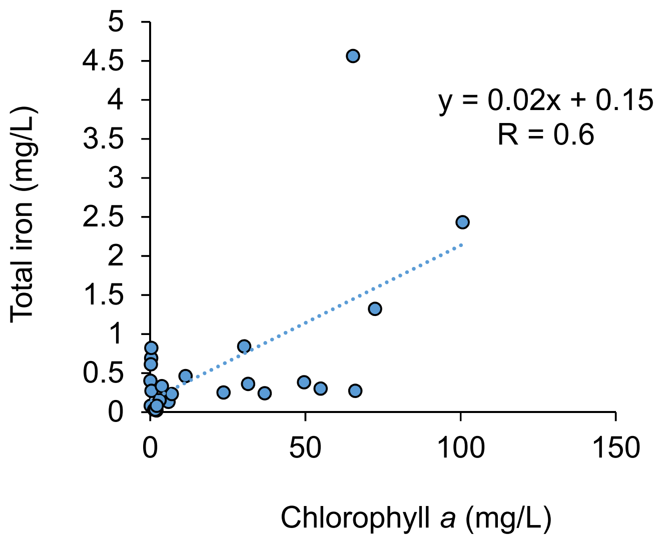

Fig. 4. Correlation between total iron and chlorophyll *a* concentration found in collected water samples (n = 26).

bacteria and algae in hydrogen peroxide dynamics (Palenik and Morel, 1988; Marsico et al., 2015; Cory et al., 2016; Zhang et al., 2016; Diaz and Plummer, 2018). There was indirect evidence that the degradation of hydrogen peroxide was the prominent process occurring during the transportation of water samples to the laboratory. The differences in hydrogen peroxide loss in filtered versus non-filtered samples appear to be attributed to bacteria; however, additional microbiological studies are needed to determine if this was by cyanobacteria or other bacteria in the samples. This result indicates the importance of removing bacteria with filtration on-site to avoid hydrogen peroxide loss (Richard et al., 2007; Vermilyea et al., 2010).

Interactions of metals with ROS have been reported previously (Nico et al., 2002; Rose et al., 2008). Among these interactions, iron has been highlighted as a key factor in the photo-Fenton-reaction in aquatic environments (Cooper and Zika, 1983; Fenton, 1894; Wilhelm, 1995). The concentrations of iron in our southwest Florida lakes ranged from 0.02 to 4.56 mg/L (median = 0.29 mg/L). These were higher than previously reported ranges in most freshwater lakes (Dimberg and Bryhn, 2015; Verschoor et al., 2017), but lower than concentrations found in Lake James, Canada (Patterson and Kumar, 2000). There was a strong positive correlation (R = 0.6, P = 0.001, n = 26) between chlorophyll *a* and total iron concentrations in the samples and over half of the iron was in the cyanobacterial cells. These findings are in line with other studies in which iron is a limiting factor in cyanobacterial blooms in nutrient-rich freshwater lakes (Imai et al., 1999; Twiss et al., 2000, Alexova et al., 2011; Xing et al., 2014). These studies also stressed that when freshwater lakes have sufficiently high nitrogen and phosphorus levels to support cyanobacterial blooms, no blooms occur when iron is limited (Utkilen and Gjølme, 1995; Alexova et al., 2011; Xing et al., 2014). During cyanobacterial growth, iron-dependent enzymes, regulated by intracellular photosynthetic thylakoid membranes, are able to control iron homeostasis within the cells (Gantt, 1994; Xing et al., 2007), and this is pivotal to facilitating photosynthetic electron transfer in PSII (Zouni et al., 2001; Kamiya and Shen, 2003; Keren et al., 2004).

Although the blooms of *Microcystis aeruginosa* have been documented in various climate zones worldwide, *M. aeruginosa* dominates more in tropical and subtropical areas where this cyanobacterium can grow rapidly with moderate temperature and strong sunlight (Bigham et al., 2009; Paerl et al., 2011; Deng et al., 2014; Mowe et al., 2015). Lake Okeechobee, FL, USA, is one of the primary sources of freshwater and the largest lake in the southeastern United States (Flaig and Reddy, 1995; Aumen and Havens, 1998). For many decades, Lake Okeechobee has been reported being subjected to intensifying *M. aeruginosa* bloom events, especially during the wet season when temperatures are high and nutrient loading is prominent (Kramer et al., 2018). The high loading of nutrients from the watershed and the discharge of water from Lake Okeechobee through the C-44 (St. Lucie River) and the C-43 canals has been speculated as a major cause of widespread blooms in estuaries at both coasts (Kramer et al., 2018). The most recent bloom event occurred in the Caloosahatchee River in 2018 and led, at one point, to a declaration of a state of emergency in Florida due to social-economic and health impacts (Fig. 5a and b). The Florida Department of Environmental Protection data showed that 71% of microcystin samples in the Caloosahatchee River exceeded the World Health Organization (WHO) recommended guideline (1998) of 1 µg/L for drinking water (WHO, 2004). Additionally, 43% of the samples exceeded the recreational guidance value of 20 µg/L on recreational water (WHO, 2003) (Fig. 5c and d). The level of microcystin was highest in the locations of the middle of the river (Fig. 5c). The microcystin concentration was found to be high in the beginning and at the end of blooms (Fig. 5d). We did not find any correlation (R = 0.39, P = 0.38, n = 7) between hydrogen peroxide concentrations and microcystin concentrations (Table 4).

Overall, our study demonstrated the effectiveness of the microelectrode approach in the study of hydrogen peroxide dynamics in subtropical freshwater ecosystems. Our study also showed a strong association of cyanobacterial blooms to hydrogen peroxide dynamics. The

Table 4
Microcystin and hydrogen peroxide concentrations in water collected from two lakes and five different sites along the Caloosahatchee River.

Location	Coordinates	Date (m/d/y)	Time	Hydrogen peroxide[b] (µM)	Microcystin (µg/L)	Chl *a* (µg/L)	Iron (mg/L)	Temp (°C)	DO (mg/L)	pH
Lake San Carlos	26°28′44″N 81°48′59″W	11/8/2017	9:10AM	2.78	2.60	90.5	7.71	24.6	1.2	8.5
Devitt Lake	26°26′39″N 82°2′57″W	8/27/2017	12:00PM	1.28	0.04	8.3	0.31	30.3	9.0	8.5
Alva Bridge[a]	26°42′50″N 81°36′36″W	6/27/2018	2:00PM	0.83	308.07	100.7	2.43	31.0	1.6	7.1
Fort Denaud Bridge[a]	26°44′40″N 81°30′37″W	6/27/2018	10:00AM	0.27	450.51	72.5	1.32	32.4	3.0	7.7
Rosen Park[a]	26°37′26″N 81°55′21″W	7/24/2018	2:00PM	5.07	24.00	65.4	4.56	30.4	5.5	7.9
Alva Bridge	26⁰42′45″N 81⁰36′35″W	11/12/2018	12:00PM	0.24	0.04	1.5	0.13	26.5	5.1	7.5
Hickey Creek	26°42′55″N 81°40′21″W	11/12/2018	2:00PM	0.85	5.45	17.2	2.35	29.0	7.5	6.1

[a] Some water analysis data are adapted from Table 2. [b]Hydrogen peroxide data are from filtered surface water samples. Total iron and all water quality data measured by the YSI sensor are shown as the mean of triplicate measurements. Hydrogen peroxide data represent the mean of six measurements. Microcystin and chlorophyll *a* data are a single measurement of each sample.

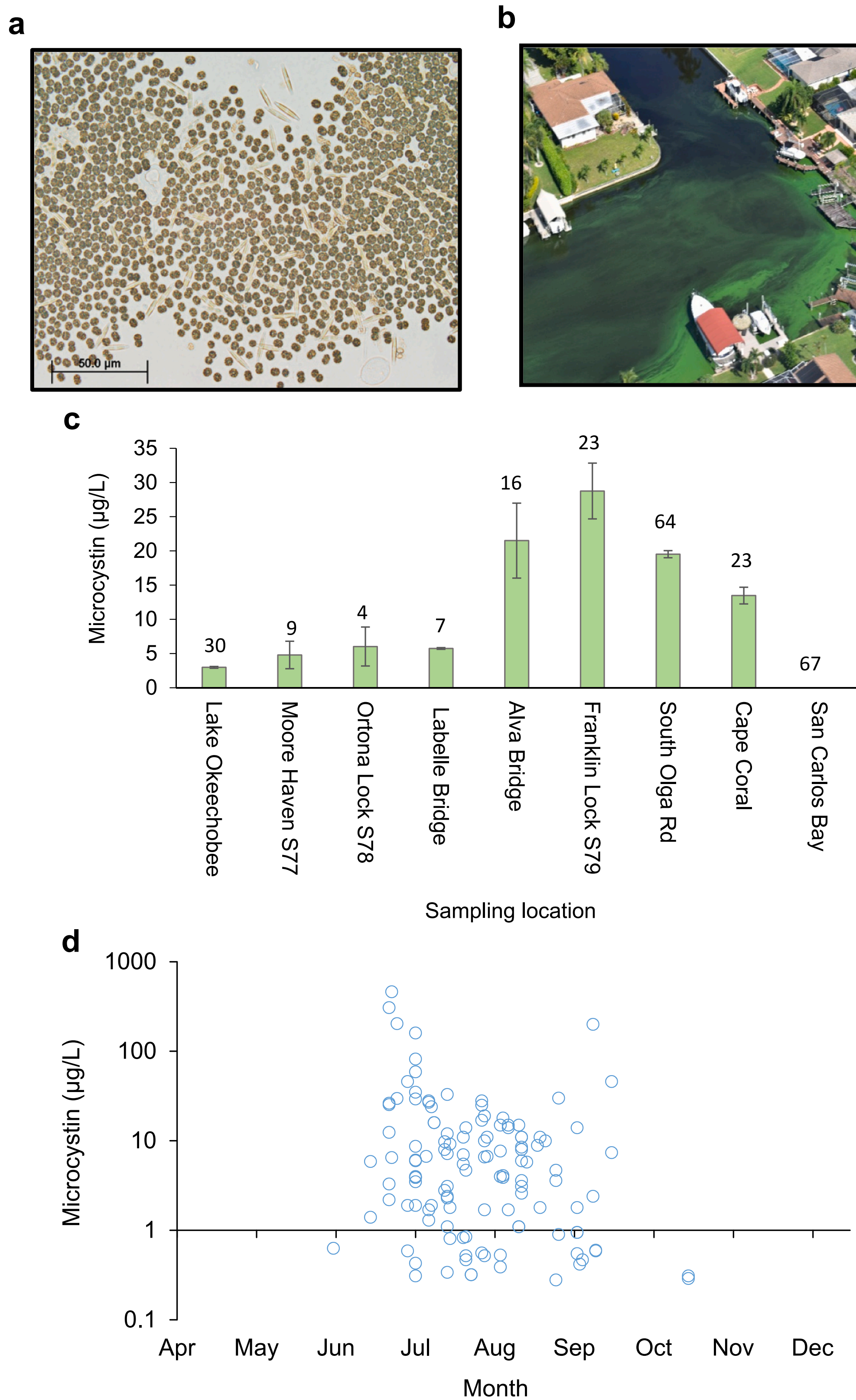

Fig. 5. 2018 harmful algal bloom events in Lake Okeechobee and the Caloosahatchee River. (a) Microscopic image of *Microcystis aeruginosa* and diatoms of the genus *Navicula* found in the Caloosahatchee River, (b) aerial image of the bloom in Cape Coral, FL, (c) microcystin concentrations shown as means and standard errors (n = 243) from sites starting from Lake Okeechobee to the downstream of the Caloosahatchee River (i.e. San Carlos Bay), and (d) the monthly changes of microcystin concentrations. Microcystin data are from Florida Algal Bloom Sample Collection View operated by the Florida Department of Environmental Protection.

use of hydrogen peroxide for algal control was tested for the first time in Netherlands waters (Matthijs et al., 2012) and is a promising algal control approach because hydrogen peroxide does not last long in aquatic environments and is degraded into water and oxygen (i.e. no harmful byproducts are produced). Well-managed hydrogen peroxide treatment is not thought to harm aquatic life (e.g. zooplankton, insects and fish) because cyanobacteria are more sensitive to hydrogen peroxide than eukaryotic phytoplankton (Drábková et al., 2007; Barrington and Ghadouani, 2008; Matthijs et al., 2012; Barrington et al., 2013). Hydrogen peroxide mitigation strategies can, therefore, stimulate the rapid succession of phytoplankton populations from HAB species to non-harmful species, which are readily consumed in classic/microbial food chains. Routine measurement of hydrogen peroxide may have a value of cyanobacterial bloom prediction. Cory and colleagues (2016) documented that hydrogen peroxide concentrations of surface water in Lake Erie reached the highest level right before a large bloom was formed. Therefore, measurements of hydrogen peroxide along with seasonal and spatial dynamics of cyanobacterial blooms and understanding of the biological and chemical process of production and degradation of hydrogen peroxide may provide a valuable framework for future water management.

Declaration of Competing Interest

None.

Acknowledgments

We thank Heather Gienapp the Lee County Recreation and Park supervisor for permitting us to get access to Six Mile Cypress Slough Preserve. We also thank Terry Matherin for permitting us to use his backyard during fieldwork in Lake San Carlos. We are indebted to Dr. Ernesto Lasso de la Vega at Lee County Hyacinth Control District for nutrient analysis. We thank Dr. H. Dail Laughinghouse IV at the University of Florida for algae identification. We thank James Evans for providing an aerial cyanobacterial bloom image. We thank Dr. Serge Thomas for his fieldwork arrangement. We are grateful to Haruka Urakawa for the provision of water analysis and the preparation of fieldwork. We thank fellow students Megan Feeney and Gabrianna Andrews for their assistance during fieldwork and analyzing samples.

Funding information

This research was supported by the US National Science Foundation, Division of Environmental Biology Ecosystem Science Cluster grant DEB-1664052 to HU, EM and MP. The study was also partially supported by the Blair Foundation Environmental Sciences Scholarship to LN and TH through the FGCU Whitaker Center, and the Student Associates for a Greener Environment (SAGE) grant, the FGCU Center for Environmental and Sustainability Education to JS.

References

Alexova, R., Fujii, M., Birch, D., Cheng, J., Waite, T.D., Ferrari, B.C., Neilan, B.A., 2011. Iron uptake and toxin synthesis in the bloom-forming *Microcystis aeruginosa* under iron limitation. Environ. Microbiol. 13 (4), 1064–1077.
Amouroux, D., Donard, O.F., 1995. Hydrogen peroxide determination in estuarine and marine waters by flow injection with fluorescence detection. Oceanol. Acta 18 (3), 353–361.
Aumen, N.G., Havens, K.E., 1998. Okeechobee, Lake (Florida) Okeechobee Lake, Florida, USA: Human impacts, research, and lake restoration. In: Encyclopedia of Hydrology and Lakes. Springer, Dordrecht, pp. 505-506.
Barrington, D.J., Ghadouani, A., 2008. Application of hydrogen peroxide for the removal of toxic cyanobacteria and other phytoplankton from wastewater. Environ. Sci. Technol. 42 (23), 8916–8921.
Barrington, D.J., Reichwaldt, E.S., Ghadouani, A., 2013. The use of hydrogen peroxide to remove cyanobacteria and microcystins from waste stabilization ponds and hypereutrophic systems. Ecol. Eng. 50, 86–94.
Bigham, D.L., Hoyer, M.V., Canfield Jr., D.E., 2009. Survey of toxic algal (microcystin) distribution in Florida Lakes. Lake Reservoir Manage. 22, 264–275.
Bowie, A.R., Lannuzel, D., Remenyi, T.A., Wagener, T., Lam, P.J., Boyd, P.W., Guieu, C., Townsend, A.T., Trull, T.W., 2009. Biogeochemical iron budgets of the Southern Ocean south of Australia: decoupling of iron and nutrient cycles in the subantarctic zone by the summertime supply. Global Biogeochem. Cycles 23 (4). https://doi.org/10.1029/2009GB003500.
Claiborn, C.S., Aneja, V.P., 1991. Measurements of atmospheric hydrogen peroxide in the gas phase and in cloud water at Mt Mitchell, North Carolina. J. Geophys. Res. Atmos. 96 (D10), 18771–18787.
Cooper, W.J., Lean, D.R.S., 1992. Hydrogen peroxide dynamics in marine and fresh water systems. Encyclopedia Earth Syst. Sci. 2, 527–535.
Cooper, W.J., Lean, D.R., 1989. Hydrogen peroxide concentration in a northern lake: photochemical formation and diel variability. Environ. Sci. Technol. 23 (11), 1425–1428.
Cooper, W.J., Saltzman, E.S., Zika, R.G., 1987. The contribution of rainwater to variability in surface ocean hydrogen peroxide. J. Geophys. Res. Oceans 92 (C3), 2970–2980.
Cooper, W.J., Zika, R.G., Petasne, R.G., Plane, J.M., 1988. Photochemical formation of hydrogen peroxide in natural waters exposed to sunlight. Environ. Sci. Technol. 22 (10), 1156–1160.
Cooper, W.J., Zika, R.G., 1983. Photochemical formation of hydrogen peroxide in surface and ground waters exposed to sunlight. Science 220, 711–712.
Cory, R.M., Davis, T.W., Dick, G.J., Johengen, T., Denef, V.J., Berry, M.A., Page, S.E., Watson, S.B., Yuhas, K., Kling, G.W., 2016. Seasonal dynamics in dissolved organic matter, hydrogen peroxide, and cyanobacterial blooms in Lake Erie. Front. Mar. Sci. 3, 54.
Deng, J., Qin, B., Paerl, H.W., Zhang, Y., Ma, J., Chen, Y., 2014. Earlier and warmer springs increase cyanobacterial (*Microcystis* spp.) blooms in subtropical Lake Taihu, China. Freshwater Biol. 59 (5), 1076–1085.
Diaz, J.M., Plummer, S., 2018. Production of extracellular reactive oxygen species by phytoplankton: past and future directions. J. Plankton Res. 40 (6), 655–666.
Dimberg, P.H., Bryhn, A.C., 2015. Predicting total nitrogen, total phosphorus, total organic carbon, dissolved oxygen and iron in deep waters of Swedish lakes. Environ. Model. Assess. 20 (5), 411–423.
Drábková, M., Admiraal, W., Maršálek, B., 2007. Combined exposure to hydrogen peroxide and light selective effects on cyanobacteria, green algae, and diatoms. Environ. Sci. Technol. 41 (1), 309–314.
Eberhardt, A.M., Pedroni, V., Volpe, M., Ferreira, M.L., 2004. Immobilization of catalase from *Aspergillus niger* on inorganic and biopolymeric supports for H_2O_2 decomposition. Appl. Catal. B 47 (3), 153–163.
Fenton, H.J.H., 1894. LXXIII.—Oxidation of tartaric acid in presence of iron. J. chem. Soc. Trans. 65, 899–910.
Flaig, E.G., Reddy, K.R., 1995. Fate of phosphorus in the Lake Okeechobee watershed, Florida, USA: overview and recommendations. Ecol. Eng. 3–4 (5), 127–142.
Fujiwara, K., Takeda, K., Kumamoto, Y.I., 1995. Generations of carbonyl sulfide and hydrogen peroxide in the Seto Inland Sea. In: Sakai, H., Nozaki Y. (Eds.), Photochemical reactions progressing in the coastal seawater Biogeochemical Processes and Ocean Flux in the Western Pacific. pp. 101–127. Terra Scientific Publishing Company (Tokyo), 1995.
Fujiwara, K., Ushiroda, T., Takeda, K., Kumamoto, Y.I., Tsubota, H., 1993. Diurnal and seasonal distribution of hydrogen peroxide in seawater of the Seto Inland Sea. Geochem. J. 27 (2), 103–115.
Gantt, E., 1994. Supramolecular membrane organization. In: The Molecular Biology of Cyanobacteria. Springer, Dordrecht, pp. 119–138.
García, P.E., Queimaliños, C., Diéguez, M.C., 2019. Natural levels and photo-production rates of hydrogen peroxide (H_2O_2) in Andean Patagonian aquatic systems: Influence of the dissolved organic matter pool. Chemosphere 217, 550–557.
Gimeno, P., Bousquet, C., Lassu, N., Maggio, A.F., Civade, C., Brenier, C., Lempereur, L., 2015. High-performance liquid chromatography method for the determination of hydrogen peroxide present or released in teeth bleaching kits and hair cosmetic products. J. Pharm. Biomed. Anal. 107, 386–393.
Häkkinen, P.J., Anesio, A.M., Granéli, W., 2004. Hydrogen peroxide distribution, production, and decay in boreal lakes. Can. J. Fish. Aquat. Sci. 61 (8), 1520–1527.
Hellpointner, E., Gäb, S., 1989. Detection of methyl, hydroxymethyl and hydroxyethyl hydroperoxides in air and precipitation. Nature 337 (6208), 631.
Holm-Hansen, O., Lorenzen, C.J., Holmes, R.W., Strickland, J.D., 1965. Fluorometric determination of chlorophyll. ICES J. Mar. Sci. 30 (1), 3–15.
Imai, A., Fukushima, T., Matsushige, K., 1999. Effects of iron limitation and aquatic humic substances on the growth of *Microcystis aeruginosa*. Can. J. Fish. Aquat. Sci. 56 (10), 1929–1937.
Kamiya, N., Shen, J.R., 2003. Crystal structure of oxygen-evolving photosystem II from *Thermosynechococcus vulcanus* at 3.7-Å resolution. Proc. Natl. Acad. Sci. 100 (1), 98–103.
Kang, C.M., Han, J.S., Sunwoo, Y., 2002. Hydrogen peroxide concentrations in the ambient air of Seoul, Korea. Atmos. Environ. 36 (35), 5509–5516.
Keren, N., Aurora, R., Pakrasi, H.B., 2004. Critical roles of bacterioferritins in iron storage and proliferation of cyanobacteria. Plant Physiol. 135 (3), 1666–1673.
Kieber, D.J., Peake, B.M., Scully, N.M., 2003. Reactive oxygen species in aquatic. UV Effects Aquatic Organisms Ecosyst. 1, 251.
Kieber, R.J., Helz, G.R., 1995. Temporal and seasonal variations of hydrogen peroxide levels in estuarine waters. Estuar. Coast. Shelf Sci. 40 (5), 495–503.
Kieber, R.J., Cooper, W.J., Willey, J.D., Avery, G.B., 2001a. Hydrogen peroxide at the Bermuda Atlantic Time Series Station. Part 1: Temporal variability of atmospheric hydrogen peroxide and its influence on seawater concentrations. J. Atmos. Chem. 39 (1), 1–13.
Kieber, R.J., Peake, B., Willey, J.D., Jacobs, B., 2001b. Iron speciation and hydrogen

peroxide concentrations in New Zealand rainwater. Atmos. Environ. 35 (34), 6041–6048.
Kramer, B.J., Davis, T.W., Meyer, K.A., Rosen, B.H., Goleski, J.A., Dick, G.J., Oh, G., Gobler, C.J., 2018. Nitrogen limitation, toxin synthesis potential, and toxicity of cyanobacterial populations in Lake Okeechobee and the St. Lucie River Estuary, Florida, during the 2016 state of emergency event. PLoS ONE 13 (5), e0196278.
Marsico, R.M., Schneider, R.J., Voelker, B.M., Zhang, T., Diaz, J.M., Hansel, C.M., Ushijima, S., 2015. Spatial and temporal variability of widespread dark production and decay of hydrogen peroxide in freshwater. Aquat. Sci. 77 (4), 523–533.
Matthijs, H.C., Visser, P.M., Reeze, B., Meeuse, J., Slot, P.C., Wijn, G., Talens, R., Huisman, J., 2012. Selective suppression of harmful cyanobacteria in an entire lake with hydrogen peroxide. Water Res. 46 (5), 1460–1472.
Miller, G.W., Morgan, C.A., Kieber, D.J., King, D.W., Snow, J.A., Heikes, B.G., Mopper, K., Kiddle, J.J., 2005. Hydrogen peroxide method intercomparision study in seawater. Mar. Chem. 97 (1–2), 4–13.
Mostofa, K.M., Liu, C.Q., Sakugawa, H., Vione, D., Minakata, D., Wu, F., 2013. Photoinduced and microbial generation of hydrogen peroxide and organic peroxides in natural waters. In: Photobiogeochemistry of Organic Matter. Springer, Berlin, Heidelberg, pp. 139–207.
Mowe, M.A., Mitrovic, S.M., Lim, R.P., Furey, A., Yeo, D.C., 2015. Tropical cyanobacterial blooms: a review of prevalence, problem taxa, toxins and influencing environmental factors. J. Limnol. 74 (2). https://doi.org/10.4081/jlimnol.2014.1005.
Nico, P.S., Anastasio, C., Zasoski, R.J., 2002. Rapid photo-oxidation of Mn (II) mediated by humic substances. Geochim. Cosmochim. Acta 66 (23), 4047–4056.
Olasehinde, E.F., Makino, S., Kondo, H., Takeda, K., Sakugawa, H., 2008. Application of Fenton reaction for nanomolar determination of hydrogen peroxide in seawater. Anal. Chim. Acta 627 (2), 270–276.
Paerl, H.W., Hall, N.S., Calandrino, E.S., 2011. Controlling harmful cyanobacterial blooms in a world experiencing anthropogenic and climatic-induced change. Sci. Total Environ. 409 (10), 1739–1745.
Palenik, B., Morel, F.M.M., 1988. Dark production of H_2O_2 in the Sargasso Sea. Limnol. Oceanogr. 33 (6part2), 1606–1611.
Patterson, B.D., MacRae, E.A., Ferguson, I.B., 1984. Estimation of hydrogen peroxide in plant extracts using titanium (IV). Anal. Biochem. 139 (2), 487–492.
Patterson, C.P., Myers, J., 1973. Photosynthetic production of hydrogen peroxide by *Anacystis nidulans*. Plant Physiol. 51 (1), 104–109.
Patterson, R.T., Kumar, A., 2000. Assessment of arcellacean (thecamoebian) assemblages, species, and strains as contaminant indicators in James Lake, Northeastern Ontario, Canada. J. Foraminiferal Res. 30 (4), 310–320.
Petasne, R.G., Zika, R.G., 1997. Hydrogen peroxide lifetimes in south Florida coastal and offshore waters. Mar. Chem. 56 (3–4), 215–225.
Pflaumer, A.L., 2016. Hydrogen peroxide in eutrophic Lake Taihu, China: Addition effects on phytoplankton and diel variability in natural concentrations (Doctoral dissertation. The University of North Carolina at Chapel Hill).
Richard, L.E., Peake, B.M., Rusak, S.A., Cooper, W.J., Burritt, D.J., 2007. Production and decomposition dynamics of hydrogen peroxide in freshwater. Environ. Chem. 4 (1), 49–54.
Roncel, M., Navarro, J.A., Miguel, A., 1989. Coupling of solar energy to hydrogen peroxide production in the cyanobacterium *Anacystis nidulans*. Appl. Environ. Microbiol. 55 (2), 483–487.
Rose, A.L., Webb, E.A., Waite, T.D., Moffett, J.W., 2008. Measurement and implications of nonphotochemically generated superoxide in the equatorial Pacific Ocean. Environ. Sci. Technol. 42 (7), 2387–2393.
Sakugawa, H., Kaplan, I.R., Tsai, W., Cohen, Y., 1990. Atmospheric hydrogen peroxide. Environ. Sci. Technol. 24 (10), 1452–1462.
Scully, N.M., McQueen, D.J., Lean, D.R.S., 1996. Hydrogen peroxide formation: the interaction of ultraviolet radiation and dissolved organic carbon in lake waters along a 43–75 N gradient. Limnol. Oceanogr. 41 (3), 540–548.
Sinel'nikov, V.E., 1971. Hydrogen peroxide level in river water, and methods for detecting it. Gibrobiol Zh 7, 115–119.
Shariati-Rad, M., Irandoust, M., Salarmand, N., 2015. Development of a Spectrophotometric Method for Determination of Hydrogen Peroxide using Response Surface Methodology. Austin J. Anal. Pharmaceutical Chem. 2 (5), 1–6.
Steinberg, S.M., 2013. High-performance liquid chromatography method for determination of hydrogen peroxide in aqueous solution and application to simulated Martian soil and related materials. Environ. Monit. Assess. 185 (5), 3749–3757.
Sun, W., Jiang, H., Jiao, K., 2005. Electrochemical determination of hydrogen peroxide using o-dianisidine as substrate and hemoglobin as catalyst. J. Chem. Sci. 117 (4), 317–322.
Takahashi, A., Hashimoto, K., Kumazawa, S., Nakayama, T., 1999. Determination of hydrogen peroxide by high-performance liquid chromatography with a cation-exchange resin gel column and electrochemical detector. Anal. Sci. 15 (5), 481–483.
Tanner, P.A., Wong, A.Y.S., 1998. Spectrophotometric determination of hydrogen peroxide in rainwater. Anal. Chim. Acta 370 (2–3), 279–287.
Twiss, M.R., Auclair, J.C., Charlton, M.N., 2000. Erratum: An investigation into iron-stimulated phytoplankton productivity in epipelagic Lake Erie during thermal stratification using trace metal clean techniques. Can. J. Fisheries Aquatic Sci. 57 (4), 870.
Urakawa, H., Bernhard, A.E., 2017. Wetland management using microbial indicators. Ecol. Eng. 108, 456–476.
Urban, S., Weltin, A., Flamm, H., Kieninger, J., Deschner, B.J., Kraut, M., Dittmeyer, R., Urban, G.A., 2018. Electrochemical multisensor system for monitoring hydrogen peroxide, hydrogen and oxygen in direct synthesis micro-reactors. Sens. Actuators, B 273, 973–982.
Utkilen, H., Gjølme, N.I.N.A., 1995. Iron-stimulated toxin production in *Microcystis aeruginosa*. Appl. Environ. Microbiol. 61 (2), 797–800.
Vermilyea, A.W., Paul Hansard, S., Voelker, B.M., 2010. Dark production of hydrogen peroxide in the Gulf of Alaska. Limnol. Oceanogr. 55 (2), 580–588.
Verschoor, M.J., Powe, C.R., McQuay, E., Schiff, S.L., Venkiteswaran, J.J., Li, J., Molot, L.A., 2017. Internal iron loading and warm temperatures are preconditions for cyanobacterial dominance in embayments along Georgian Bay, Great Lakes. Can. J. Fish. Aquat. Sci. 74 (9), 1439–1453.
Wilhelm, S.W., 1995. Ecology of iron-limited cyanobacteria: a review of physiological responses and implications for aquatic systems. Aquat. Microb. Ecol. 9 (3), 295–303.
World Health Organization, 1998. Guidelines for drinking-water quality. Vol. 2, Health criteria and other supporting information: addendum (No. WHO/EOS/98.1). Geneva: World Health Organization.
World Health Organization, 2003. Guidelines for safe recreational water environments: Coastal and fresh waters Vol. 1 World Health Organization.
World Health Organization, 2004. Guidelines for drinking-water quality: recommendations (Vol. 1). World Health Organization.
Xing, W., Huang, W.M., Li, D.H., Liu, Y.D., 2007. Effects of iron on growth, pigment content, photosystem II efficiency, and siderophores production of *Microcystis aeruginosa* and *Microcystis wesenbergii*. Curr. Microbiol. 55 (2), 94–98.
Xing, W., Huang, W., Liu, G., Liu, Y., 2014. Effects of temperature, light, nitrate and ammonium on growth and photosynthesis of *Microcystis aeruginosa* (cyanobacteria) under iron-limited and iron-replete conditions. Fresenius Environ. Bull. 23 (8 A), 1934–1941.
Yeoman, K., Jiang, B., Mitsch, W.J., 2017. Phosphorus concentrations in a Florida Everglades water conservation area before and after El Niño events in the dry season. Ecol. Eng. 108, 391–395.
Zhang, T., Hansel, C.M., Voelker, B.M., Lamborg, C.H., 2016. Extensive dark biological production of reactive oxygen species in brackish and freshwater ponds. Environ. Sci. Technol. 50 (6), 2983–2993.
Zhou, B., Wang, J., Guo, Z., Tan, H., Zhu, X., 2006. A simple colorimetric method for determination of hydrogen peroxide in plant tissues. Plant Growth Regul. 49 (2–3), 113–118.
Zouni, A., Witt, H.T., Kern, J., Fromme, P., Krauss, N., Saenger, W., Orth, P., 2001. Crystal structure of photosystem II from *Synechococcus elongatus* at 3.8 Å resolution. Nature 409 (6821), 739.